The American Journal of Human Genetics, Volume *107*

Supplemental Data

Mutations of the Transcriptional Corepressor *ZMYM2* Cause Syndromic Urinary Tract Malformations

Dervla M. Connaughton, Rufeng Dai, Danielle J. Owen, Jonathan Marquez, Nina Mann, Adda L. Graham-Paquin, Makiko Nakayama, Etienne Coyaud, Estelle M.N. Laurent, Jonathan R. St-Germain, Lot Snijders Blok, Arianna Vino, Verena Klämbt, Konstantin Deutsch, Chen-Han Wilfred Wu, Caroline M. Kolvenbach, Franziska Kause, Isabel Ottlewski, Ronen Schneider, Thomas M. Kitzler, Amar J. Majmundar, Florian Buerger, Ana C. Onuchic-Whitford, Mao Youying, Amy Kolb, Daanya Salmanullah, Evan Chen, Amelie T. van der Ven, Jia Rao, Hadas Ityel, Steve Seltzsam, Johanna M. Rieke, Jing Chen, Asaf Vivante, Daw-Yang Hwang, Stefan Kohl, Gabriel C. Dworschak, Tobias Hermle, Mariëlle Alders, Tobias Bartolomaeus, Stuart B. Bauer, Michelle A. Baum, Eva H. Brilstra, Thomas D. Challman, Jacob Zyskind, Carrie E. Costin, Katrina M. Dipple, Floor A. Duijkers, Marcia Ferguson, David R. Fitzpatrick, Roger Fick, Ian A. Glass, Peter J. Hulick, Antonie D. Kline, Ilona Krey, Selvin Kumar, Weining Lu, Elysa J. Marco, Ingrid M. Wentzensen, Heather C. Mefford, Konrad Platzer, Inna S. Povolotskaya, Juliann M. Savatt, Natalia V. Shcherbakova, Prabha Senguttuvan, Audrey E. Squire, Deborah R. Stein, Isabelle Thiffault, Victoria Y. Voinova, Michael J.G. Somers, Michael A. Ferguson, Avram Z. Traum, Ghaleb H. Daouk, Ankana Daga, Nancy M. Rodig, Paulien A. Terhal, Ellen van Binsbergen, Loai A. Eid, Velibor Tasic, Hila Milo Rasouly, Tze Y. Lim, Dina F. Ahram, Ali G. Gharavi, Heiko M. Reutter, Heidi L. Rehm, Daniel G. MacArthur, Monkol Lek, Kristen M. Laricchia, Richard P. Lifton, Hong Xu, Shrikant M. Mane, Simone Sanna-Cherchi, Andrew D. Sharrocks, Brian Raught, Simon E. Fisher, Maxime Bouchard, Mustafa K. Khokha, Shirlee Shril, and Friedhelm Hildebrandt

Supplemental Data

Supplementary Text

Since the nuclear localization site (NLS) usually consists of one or more short sequences of positively charged lysines or arginines exposed on the protein surface, we hypothesized that a new NLS should be located in p.718-p723. To test this hypothesis, we employed immunofluoroscence of wild type and three missense mutated ZMYM2 proteins (Arg. in p.718, p.719 and p.723 mutated to Ala). The missense mutant protein (p.Arg718Ala) showed the same expression pattern as wild type in all cells with a nuclear signal, while the other two missense mutant proteins (p.Arg719Ala and p.Arg723Ala) have a mainly cytoplasmic pattern in all cells with partially nuclear signal in some cells. We therefore conclude that Arg in p.719 or p.723 mutated to Ala is sufficient to influence the nuclear localization of ZMYM2, which suggests that p.719-p723 (RLGLR) is the region of this new functional NLS.

Acknowledgements

We are grateful the families who contributed to this study. We thank the Leslie Spaneas (USA), Alana Gerald (USA), and Kassaundra Amann (USA) for person recruitment.

D.M.C. is funded by Health Research Board, Ireland (HPF-206-674), the International Pediatric Research Foundation Early Investigators' Exchange Program and the Amgen® Irish Nephrology Society Specialist Registrar Bursary. She is also funded by the Eugen Drewlo Chair for Kidney Research and Innovation at the Schulich School

of Medicine & Dentistry at Western University, London, Ontario, Canada.

D.O. and A.D.S were funded by the Wellcome Trust.

J.M. is supported by the Yale MSTP NIH T32GM007205 Training Grant and the Paul and Daisy Soros Fellowship for New Americans, and this research was supported by grants from the National Institute of Health to M.K.K. (RO1HD081379).

N.M. is supported by funding from the National Institute of Health (T32-DK007726-33) grant at Boston Children's Hospital.

A.L.G.P is supported by the Fonds de Recherche du Quebec-Sante (FRQS).

M.N. is supported by the Japan Society for the Promotion of Science.

A.T.v.d.V. (VE 969 -7) is supported by a Postdoctoral Research Fellowship from the German Research Foundation (DFG). A.V. is supported by a Manton Center for Orphan Diseases Research grant.

E.MN.L is supported by a Métropole Européenne de Lille (MEL) Research grant.

E.C. is supported by a *Marie* Skłodowska-*Curie* actions (MSCA-IF-843052).

V.K. (403877094) is supported by the Deutsche Forschungsgemeinschaft.

I.O. is supported by the German National Academic Scholarship Foundation (Studienstiftung des deutschen Volkes) and German Academic Exchange Service (DAAD). C.-H.W.W. is supported by funding from the National Institute of Health (Grant T32-GM007748).

T.M.K. was supported by a Post-Doctoral Fellowship award from the KRESCENT Program, a national kidney research training partnership of the Kidney Foundation of Canada, the Canadian Society of Nephrology, and the Canadian Institutes of Health

Research.

F.B. was supported by a fellowship grant (404527522) from the German Research Foundation (DFG).

A.J.M. was supported by an NIH Training Grant (T32DK-007726), by the 2017 Post-doctoral Fellowship Grant from the Harvard Stem Cell Institute, and by the American Society of Nephrology Lipps Research Program 2018 Polycystic Kidney Disease Foundation Jared J. Grantham Research Fellowship.

A.C.O. is supported by the NIH F32 Ruth L. Kirschstein National Research Service Award (DK122766).

I.S.P., N.V.S., V.Y.V. were supported by the Government Assignment of the Russian Ministry of Health, Assignment No. AAAA-A18-118051790107-2.

L.S.B. and S.E.F. are supported by the Netherlands Organization for Scientific Research (NWO) Gravitation Grant 24.001.006 to the Language in Interaction Consortium. Ar.V and S.E.F. are supported by the Max Planck Society.

S.S.-C. was supported by the National Institute of Health grants 1R01DK103184, 1R01DK115574, and P20DK116191.

M.B. is supported by a Canadian Institutes for Health Research (CIHR) grant (PJT-159768) and by a grant from the Kidney Foundation of Canada. A.G.G. is supported by 5 R01 DK080099. Sequencing and data processing was performed by the Broad and Yale Centers for Mendelian Genomics funded by the National Human Genome Research Institute (UM1 HG008900 to DGM and HLR and U54 HG006504 to RPL). F.H. and S.S. are supported by grants from the National Institutes of Health to FH (DK076683) and the Begg Family Foundation.

This research was supported by grants from the National Institutes of Health to R.P.L and to F.H. (DK088767).

Figure S1. Confocal microscope analysis of ZMYM2 following MYC tagged ZMYM2 transfection with wild type or mutant.

(A) Location of Myc-ZMYM2 wild type and mutant proteins in Hek293 cells.

ZMYM2 wild type (wt) and missense mutant protein were diffusely nuclear localized. The **truncated** proteins (p.Gly257fs*,p.Gln398, p.Arg540*) showed cytoplasmic pattern in all cells. However, in some cells the locations of some **truncated** proteins (p.Tyr763Glnfs*6, p.Cys812Aspfs*18, p.Asp997del,p.Cys823*, p.Gly1045Argfs*33) were partially nuclear, suggesting that the early reputative Nuclear Localization Signal (NLS) (p.1038-1049 and p.1250-1284) greatly affected the location of ZMYM2 protein, while, there should be another functional NLS between p.540 and p.763. (White bar = 15μm)

Figure S2 zmym2 Expression and Depletion in Xenopus

A Figure depicting expression of *zmym2* (referred to as *zfp198*) in *Xenopus laevis* embryos at a variety of stages (Adapted from Nielson *et al.* Dev Dyn 2010).

B Figure deposited in Xenbase by the Papalopulu lab depicting expression of *zmym2* in a stage 28 *Xenopus tropicalis* embryos.

C Expression of *zmym2* in a stage 34 *Xenopus tropicalis* embryo with sense control shown for comparison. Arrows indicate enrichment of expression in pronephros and pronephric tubule.

D Agarose gel confirming splice blocking achieved by MO injection. Upper arrowhead indicates full length product of PCR flanking exon 3 from cDNA while lower arrowhead indicated splice blocked product seen only in splice blocking MO injected embryo cDNA.

Figure S3 Sanger confirmation with segregation (if available) for each of the heterozygous mutations identified in families.

Figure S4. Luciferase reporter assay, driven by a LexA-VP16 fusion protein, to test if Gal4-ZMYM2 fusion protein for the missense mutants could repress transcription.

Lex-VP16 is transfected to activate the reporter, and then either 5 or 50ng of GAL-ZMYM2 (wild-type or mutants as indicated) are added. The transcriptional repressive activity is retained in both the wild type and missense mutant proteins.

Figure S5 Expression of *ZMYM2* and patient variant sequences in *zmym2* morphant *Xenopus* embryos identifies variants with loss of function in pronephric development.

Xenopus embryos were injected with MO at the one-cell stage. mRNA derived from either wildtype or variant *ZMYM2* was then injected at the 2-cell stage. Proximal pronephric area was scored at stage 34. MO only and MO + mRNA injected sides of embryos receiving wildtype or variant mRNA. Scale bars depict 500 μm.

Figure S6. Additional data on Zmym2 heterozygous mutant mouse model.

A. Frameshift mutation in ZMYM2+/− mouse models mutation found in individual GM1-21 (c 766_767 GT nucleotide duplication).

B. Curve of non-refluxing animals relative to pressure (centimeters representing the height of dye reservoir; bladder level= 0 cm) for wild-type (n = 25) andZMYM2+/−(n = 20) **p-value of 0.0039 was calculated using the Gehan-Breslow-Wilcoxon test for survival curves. Grey dotted area represents the average pressure at which the urethra voids +/− 1 SD.

C. Urethral voiding pressures is unaffected in ZMYM2+/− mice (student t-test).

Figure S7. Zmym2 expression in the developing mouse urinary tract

A. Immunohistofluorescence analysis of wildtype E18.5 kidneys shows low and widespread expression of Zmym2. Cytokeratin 8/18 expression highlights tissue structure. Structures labeled include: UT: ureter tip, RPC: renal progenitor cells, CD: collecting duct, PT: proximal tubules, DT: distal tubules, G: glomerulus. Yellow foci come from autofluorescent blood cells.

B. In situ hybridization of *Zmym2* in E15.5 urogenital systems of female (top) and male (bottom) mice. Images taken from GUDMAP database, Specimens: N-H79Y,N-H7CR.

This study used data from the GUDMAP database, http://www.gudmap.orgon May 26, 2020, including in situ data generated by McMahon, A. in correspondence with the following publication: Brunskill EW, Park JS, Chung E, Chen F, Magella B, Potter SS. Single cell dissection of early kidney development: multilineage priming. *Development*. 2014;141(15):3093-3101. https://doi.org/10.1242/dev.074005

C. Expression levels of Zmym2, Pax2 and Six2 in developing kidney tissues. Note: Mean values of similar samples are presented for E15.5 collecting duct (GSM1585035, GSM1585037, GSM1585042), E15.5 podocytes (GSM1585039,GSM1585036) and E15.5 proximal tubules (GSM1585040,GSM1585034), where error bars show SD. This graph was generated using RNA sequencing data of micro-dissected and FACS-sorted developing tissues, dataset ID: GSE64959.

Figure S8 Identification of a new *ZMYM2* Nuclear Localization Signal or Sequence (NLS) site.

A. Yellow highlights the positively charged lysines or arginines NLS characteristic of NLS. Green numbers indicated the 6 potential NLS are located in the region p.540 – p.763.

B. Immunofluoroscence of wild type (Wt) and the truncated ZMYM2 proteins.

C. Immunofluoroscence of wild type and three missense, mutated ZMYM2 proteins which suggests that p.719-p723 (RLGLR) is the region of this new functional NLS.

Figure S9

A) Bioluminescence Resonance Energy Transfer (BRET) assays to measure effects of ZMYM2 protein truncations on interactions with FOXP1, FOXP2 and wild-type ZMYM2.

Wild-type ZMYM2 and three different truncated constructs of ZMYM2 (pGly257*, pGln398*, pArg540*) were overexpressed as fusion proteins with YFP, and function as acceptor constructs in these assays (X-axis). Co-expressed donor constructs were either NLS (a negative control with nuclear localization signal only), FOXP1, FOXP2 or wild-type ZMYM2 constructs, in each case overexpressed as a fusion protein with Renilla

luciferase (rLuc). Bars represent the corrected mean BRET ratio ± standard deviation of three independent experiments performed in triplicate (see Methods for details). All three truncated ZMYM2 constructs showed impaired interaction with FOXP1 and FOXP2, compared with wild-type ZMYM2 interaction capacities.

B) Immunoblot analysis of constructs used in BRET assays

Western blot with whole-cell lysates expressing seven different YFP-tagged ZMYM2 constructs, probed with an anti-EGFP antibody. These constructs included wild-type, three missense variants and three stop-gain variants. Lane 1: untransfected cells; Lane 2: wild-type; lane 3: pLys649Arg; lane 4: pTyr763His; lane 5: pAsp997del; lane 6: pGly257*; lane 7: pGln398*; lane 8: pArg540*. This blot demonstrates that all ZMYM2-YFP-fusion proteins used for the BRET assays (wild-type, pGly257*, pGln398*, pArg540*) are expressed at the expected molecular weights.

Figure S10. Proximity-dependent biotin identification demonstrating the ZMYM2 protein interaction landscape or ZMYM2 interactome

The interactome shows that ZMYM2 is significantly enriched in DNA binding transcription factors, transcriptional co-repressors, and proteins linked to chromatin regulation, chromatin organization and SUMO ligase activity (p=6.7x10-05). The majority of the components involved multiple previously reported ZMYM2 interactors26: LSD1(KDM1A)-CoREST (Corum complexes 633 and 1492)27, HDAC128 and HDAC2 (Corum 632). IP-MS (immunoprecipitation coupled with mass spectrometry) analyses were identified in our ZMYM2 BioID analysis (HDAC1, HDAC2, KDM1A/LSD1, GTF2I, GSE1/KIAA0182, PHF21A/BHC80, RCOR1, RCOR2, RCOR3, ZNF217, ZMYM3 and ZMYM4)

Figure S11 ZMYM2 truncation mutant BioID Heat Map

Table S1. List of mutagenesis primers used to generate clones representing the variants identified in each family

Table S2. Twelve non-pathogenic missense heterozygous mutations in *ZMYM2* in 13 individuals from 12 families with congenital anomalies of the kidney and urinary tract.

Table S3. List of truncating heterozygous variants of *ZMYM2* that exist in gnomAD.

Table S4A. Overview of *ZMYM2* variants identified in two control cohorts of 100 families with steroid resistant nephrotic syndrome and 238 families with nephronophthisis.

Table S4B. Overview of monogenic causes identified in a cohort of 100 patients with steroid resistant nephrotic syndrome.

Table S5. Proximity-dependent biotin identification (BioID) characterizing the ZMYM2 protein interaction landscape.

Table S6. Proximity-dependent biotin identification (BioID) characterizing the ZMYM3 protein interaction landscape.

Figure S1. Confocal microscope analysis of ZMYM2 following MYC tagged ZMYM2 transfection with wild type or mutant.

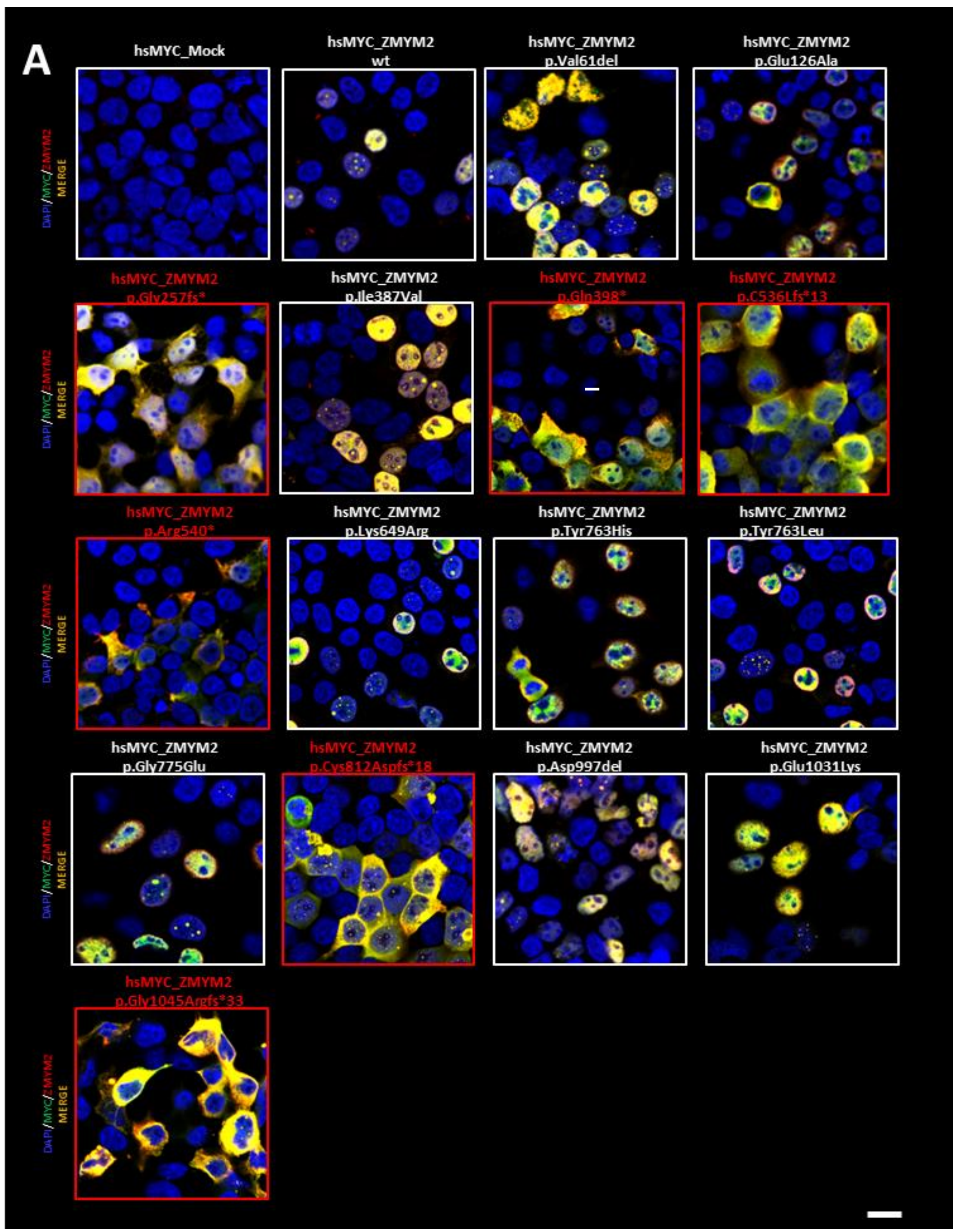

(A) Location of Myc-ZMYM2 wild type and mutant proteins in Hek293 cells. ZMYM2 wild type (wt) and missense mutant protein were diffusely nuclear localized. The **truncated** proteins (p.Gly257fs*,p.Gln398, p.Arg540*) showed cytoplasmic pattern in all cells. However, in some cells the locations of some **truncated** proteins (p.Tyr763Glnfs*6, p.Cys812Aspfs*18, p.Asp997del,p.Cys823*, p.Gly1045Argfs*33) were partially nuclear, suggesting that the early reputative Nuclear Localization Signal (NLS) (p.1038-1049 and p.1250-1284) greatly affected the location of ZMYM2 protein, while, there should be another functional NLS between p. 540 and p.763.(White bar = 15μm)

Figure S2 zmym2 Expression and Depletion in Xenopus

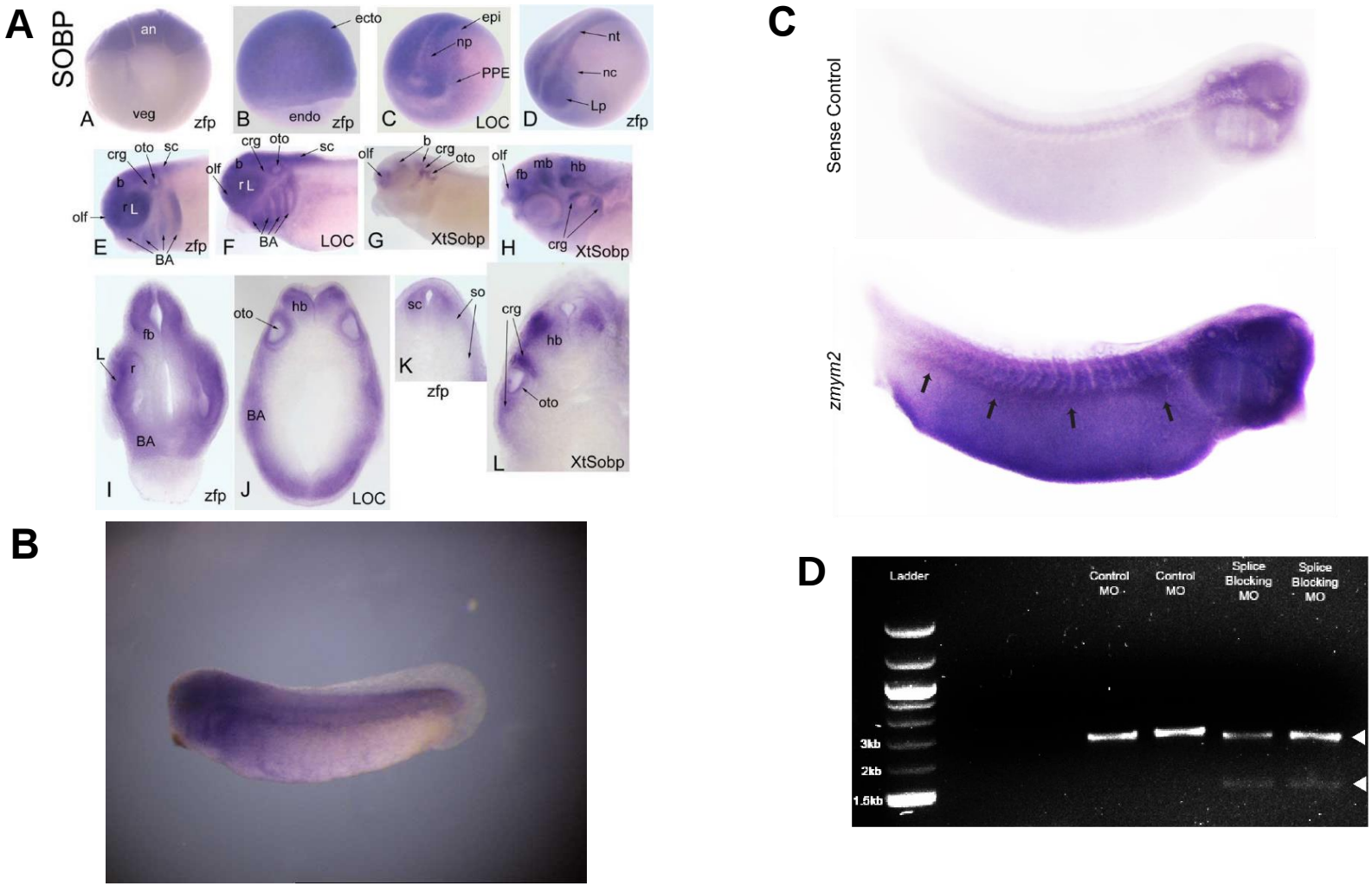

A Figure depicting expression of *zmym2* (referred to as *zfp198*) in *Xenopus laevis* embryos at a variety of stages (Adapted from Nielson *et al.* Dev Dyn 2010).
B Figure deposited in Xenbase by the Papalopulu lab depicting expression of *zmym2* in a stage 28 *Xenopus tropicalis* embryos.
C Expression of *zmym2* in a stage 34 *Xenopus tropicalis* embryo with sense control shown for comparison. Arrows indicate enrichment of expression in pronephros and pronephric tubule.
D Agarose gel confirming splice blocking achieved by MO injection. Upper arrowhead indicates full length product of PCR flanking exon 3 from cDNA while lower arrowhead indicated splice blocked product seen only in splice blocking MO injected embryo cDNA.

Figure S3. Sanger confirmation with segregation (if available) of each of the heterozygous mutations identified in families.

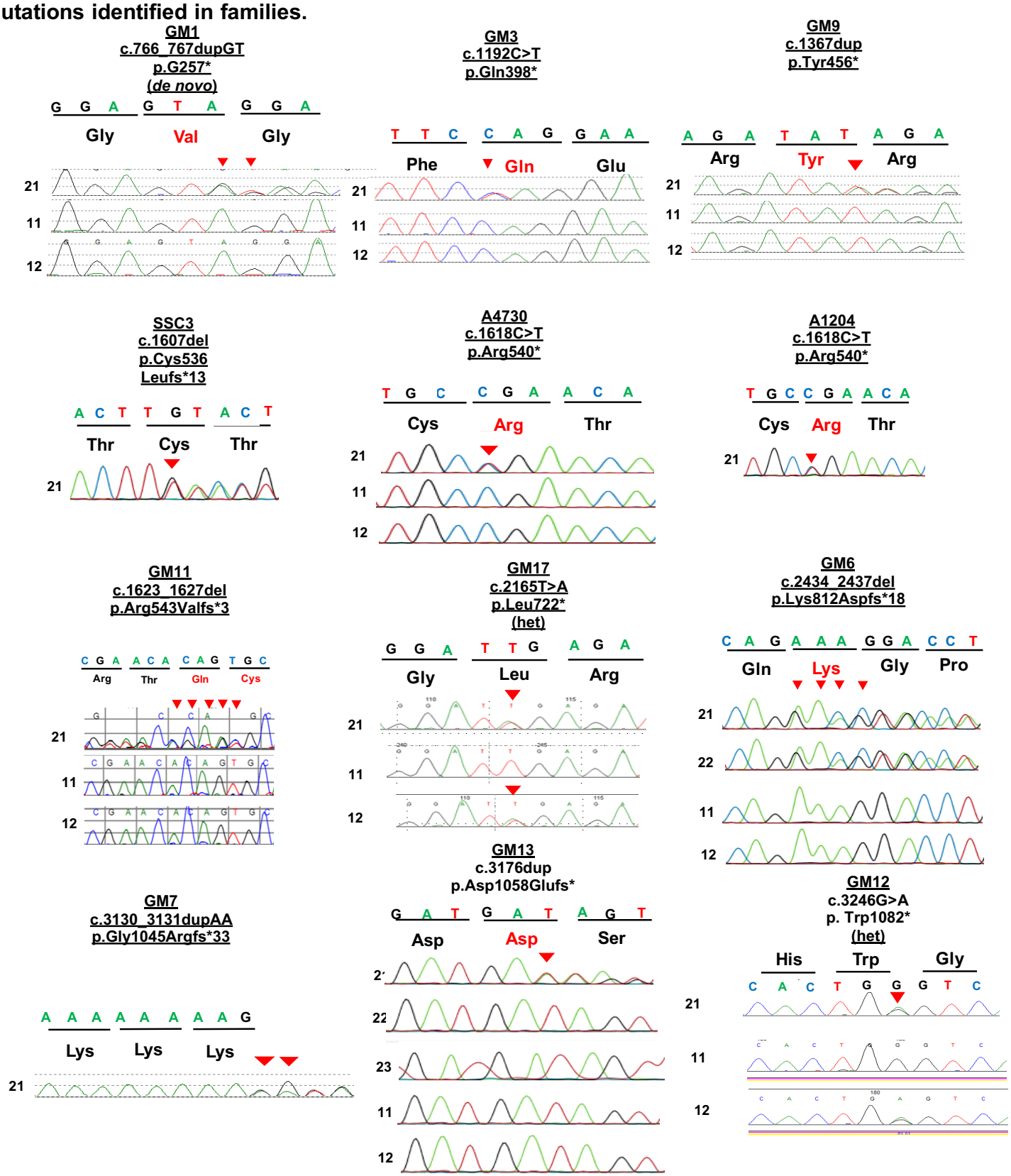

Figure S4. Luciferase reporter assay, driven by a LexA-VP16 fusion protein, to test if Gal4-ZMYM2 fusion protein could repress transcription

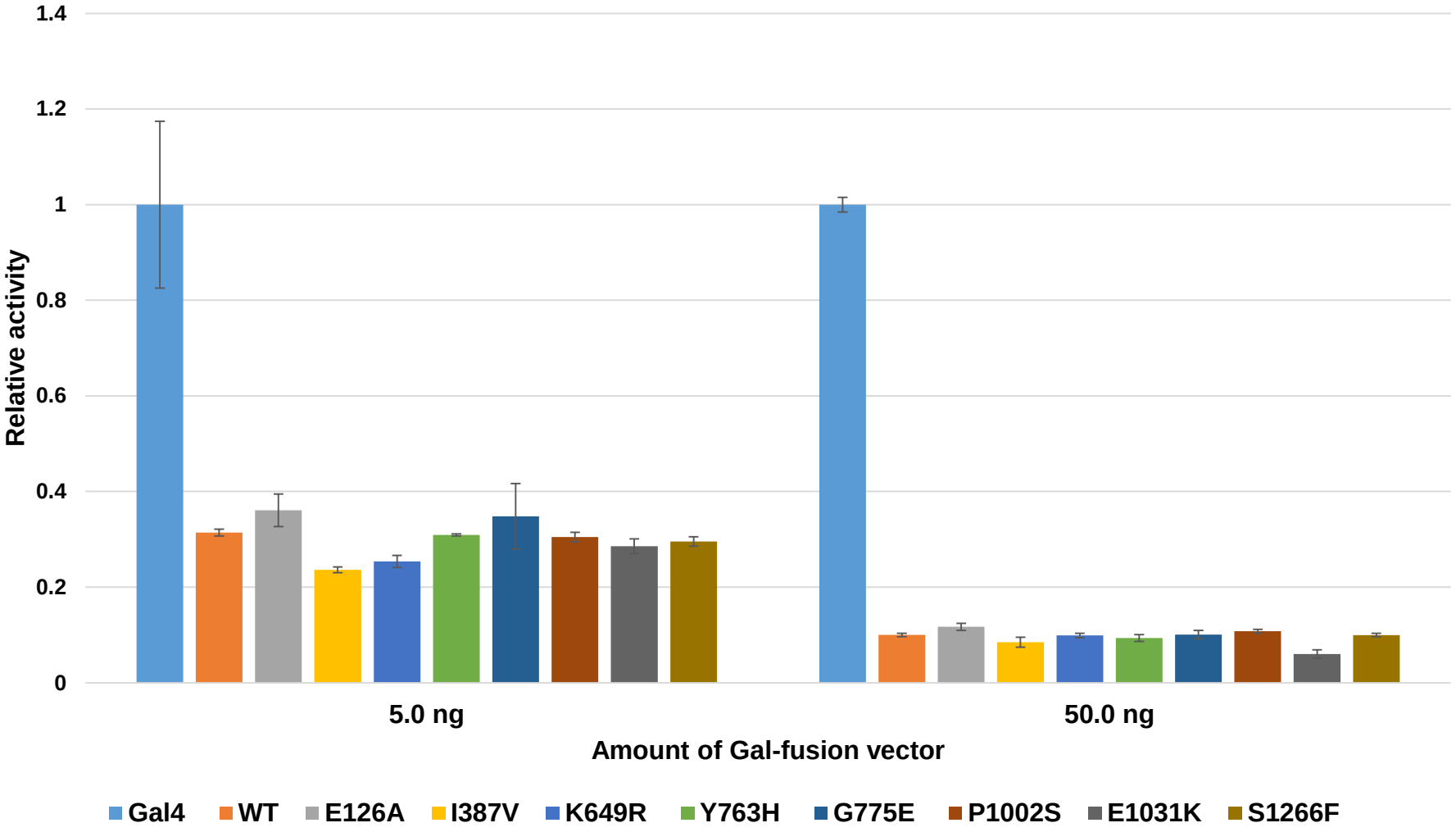

Lex-VP16 is transfected to activate the reporter, and then either 5 or 50ng of GAL-ZMYM2 (wild-type or missense mutants as indicated) are added.
The transcriptional repressive activity is retained in both the wild type and missense mutant proteins.

Figure S5. Expression of *ZMYM2* and patient variant sequences in *zmym2* morphant *Xenopus* embryos identifies variants with loss of function in pronephric development.

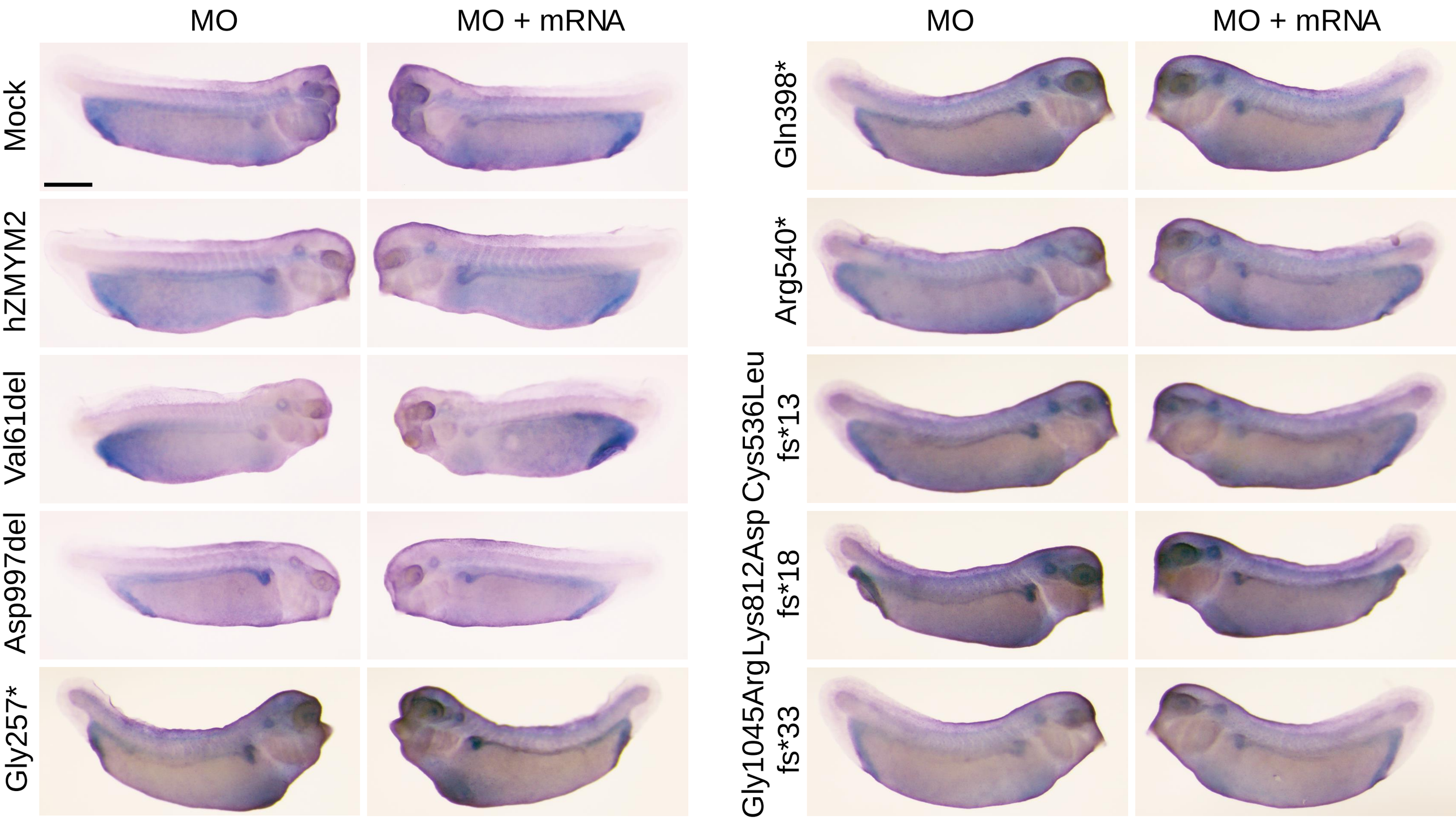

Scale bars depict 500 µm.

Figure S6. Additional data on Zmym2 heterozygous mutant mouse model.

A

Human			
WT	180	E I Q I A N V T T L E T G V S S V N D G Q L E N	205
GT dup	180	E I Q I A N V T T L E T G V *	194
Mouse			
WT	180	E I Q I A N V T T L E T G V S S V S D G Q L E S	205
GT dup	180	E I Q I A N V T T L E T G V *	194
Δ1bp	180	E I Q I A N V T T L E Q A *	193

CRISPR Cas9 cut site

B

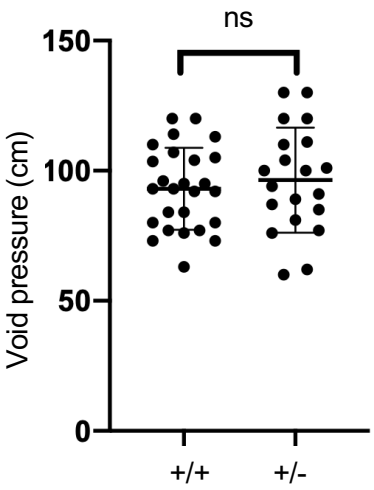

C

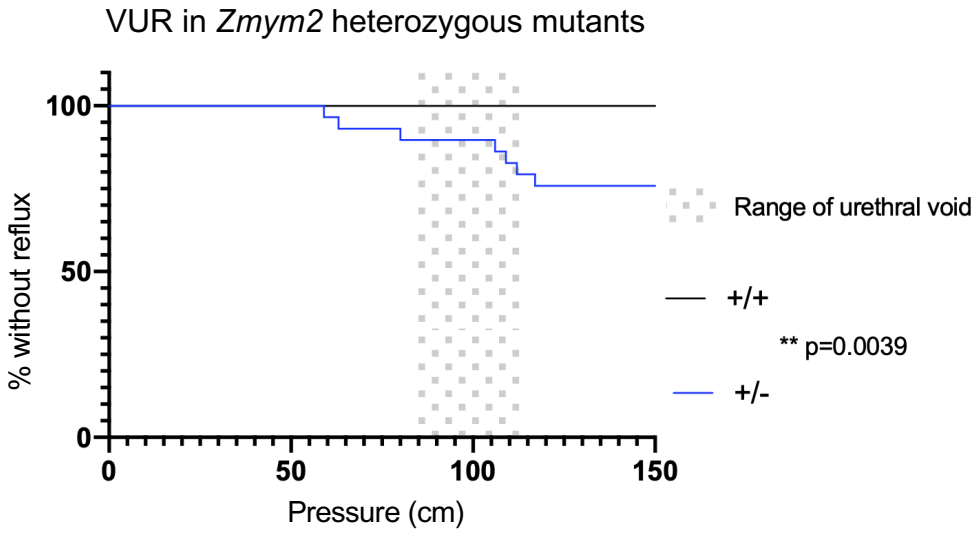

Figure S7. Zmym2 expression in the developing mouse urinary tract

A

Zmym2 ; CK8/18

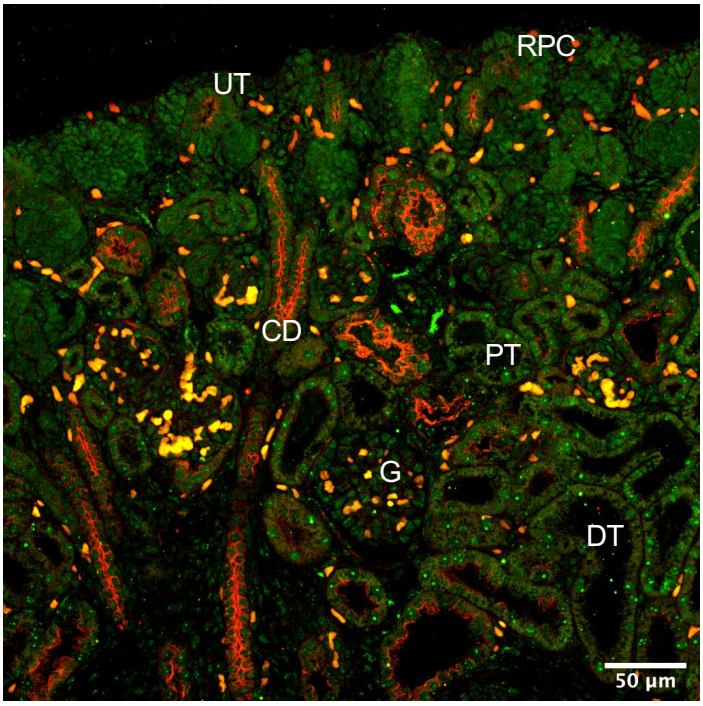

No primary control

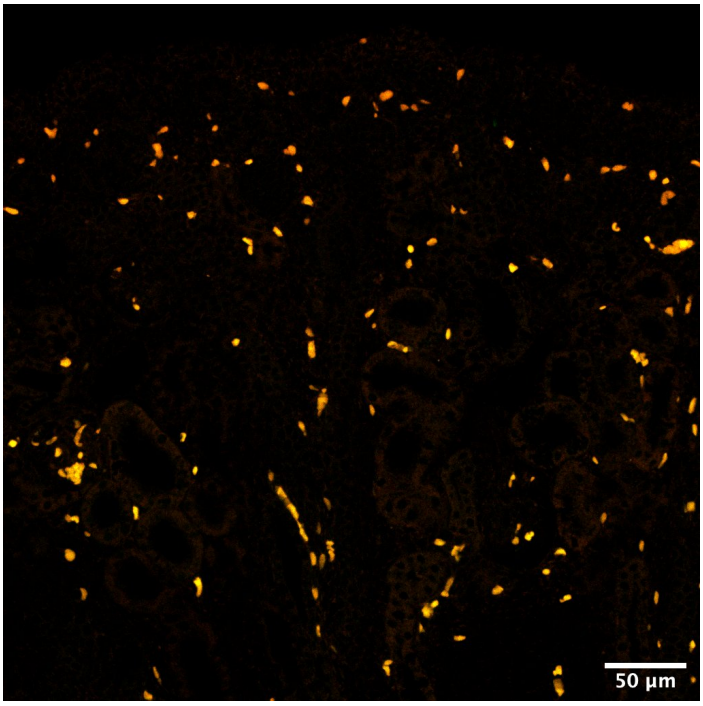

B

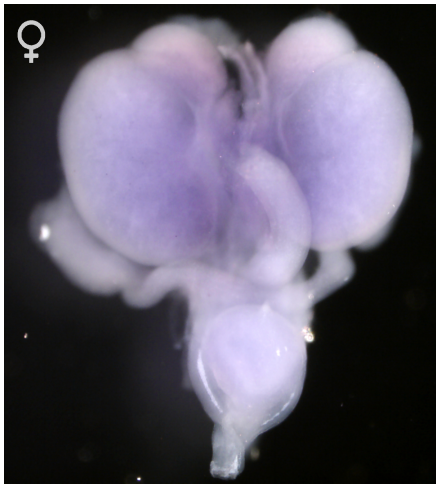

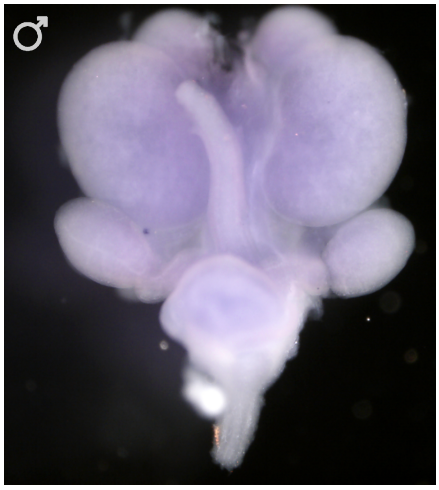

C

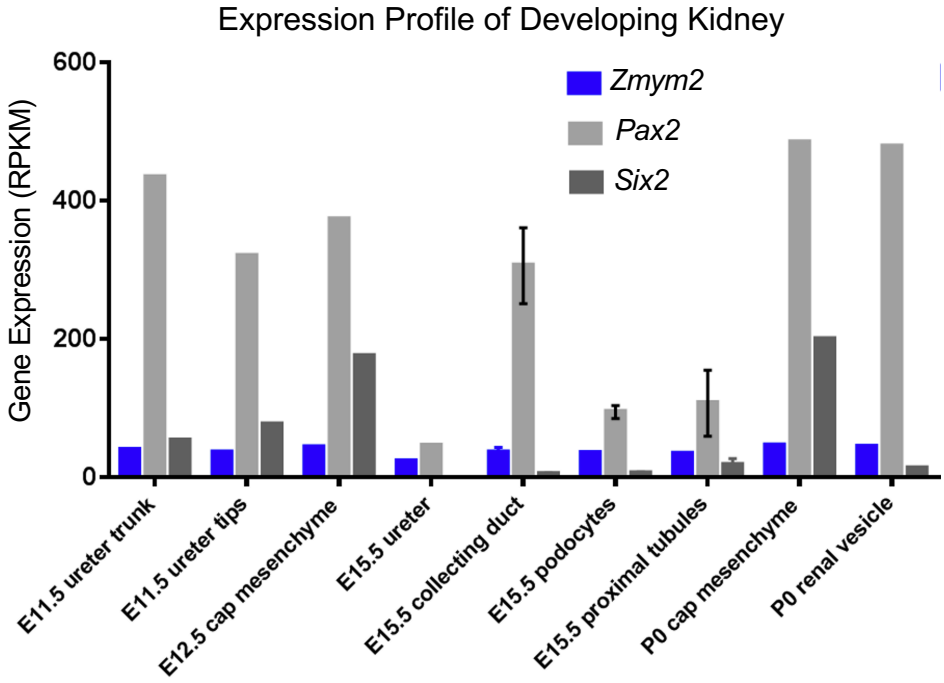

Figure S8. Identification of a new *ZMYM2* Nuclear Localization Signal or Sequence (NLS) site.

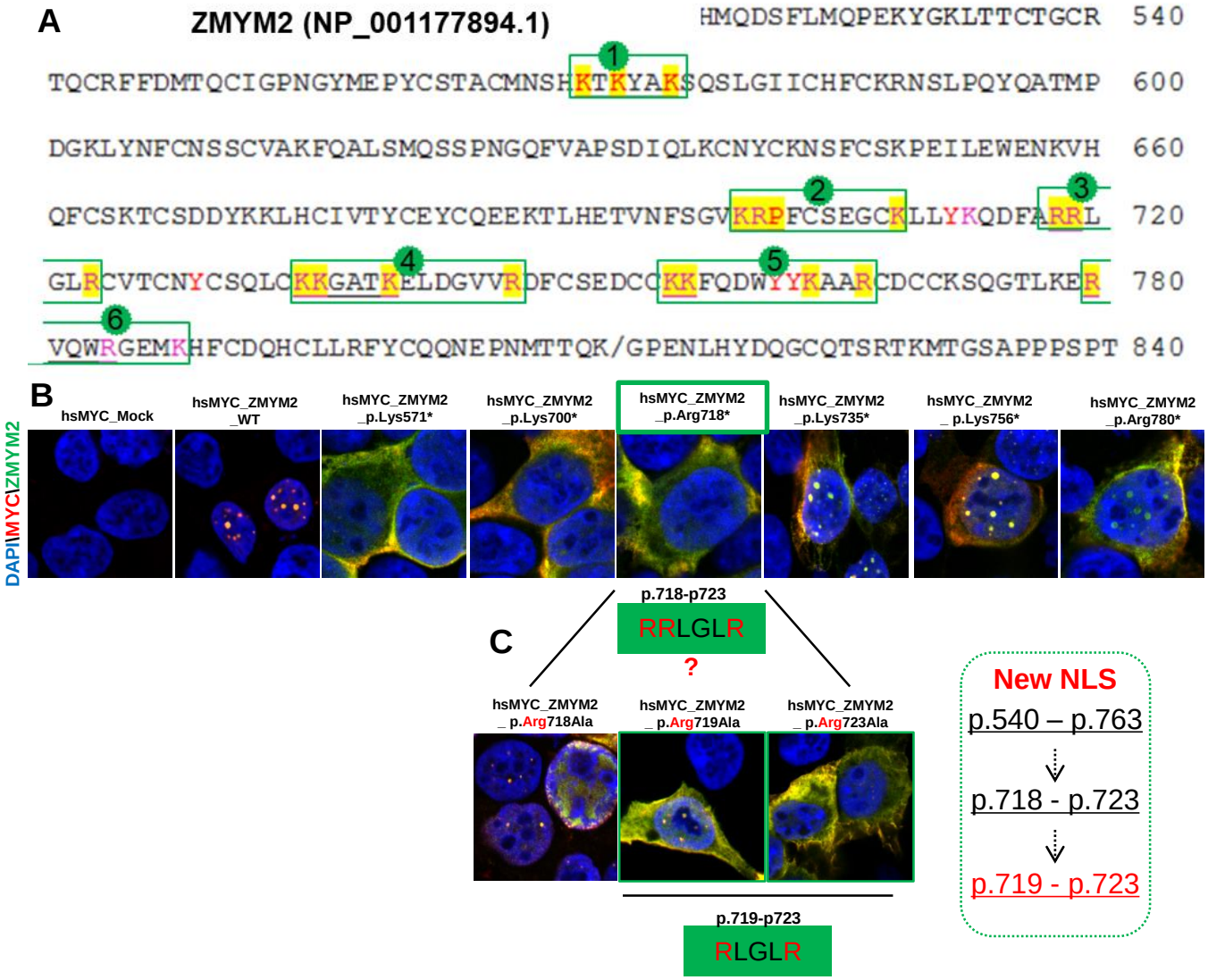

A. Yellow highlights the positively charged lysines or arginines NLS characteristic of NLS. Green numbers indicated the 6 potential NLS are located in the region p.540 – p.763.
B. Immunofluoroscence of wild type (Wt) and the truncated ZMYM2 proteins.
C. Immunofluoroscence of wild type and three missense, mutated ZMYM2 proteins which suggests that p.719-p723 (RLGLR) is the region of this new functional NLS.

Figure S9

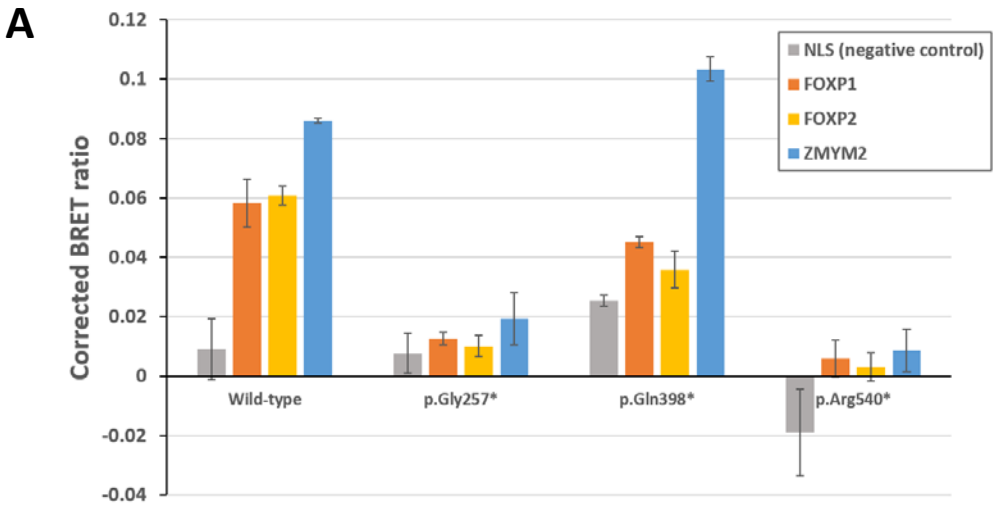

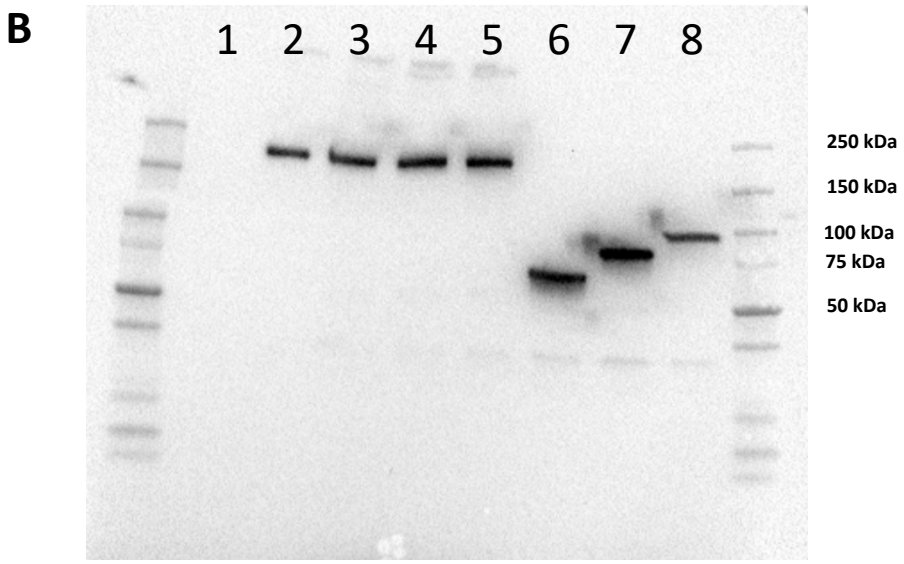

A) Bioluminescence Resonance Energy Transfer (BRET) assays to measure effects of ZMYM2 protein truncations on interactions with FOXP1, FOXP2 and wild-type ZMYM2.
Wild-type ZMYM2 and three different truncated constructs of ZMYM2 (pGly257*, pGln398*, pArg540*) were overexpressed as fusion proteins with YFP, and function as acceptor constructs in these assays (X-axis). Co-expressed donor constructs were either NLS (a negative control with nuclear localization signal only), FOXP1, FOXP2 or wild-type ZMYM2 constructs, in each case overexpressed as a fusion protein with Renilla luciferase (rLuc). Bars represent the corrected mean BRET ratio ± standard deviation of three independent experiments performed in triplicate (see Methods for details). All three truncated ZMYM2 constructs showed impaired interaction with FOXP1 and FOXP2, compared with wild-type ZMYM2 interaction capacities.

B) Immunoblot analysis of constructs used in BRET assays
Western blot with whole-cell lysates expressing seven different YFP-tagged ZMYM2 constructs, probed with an anti-EGFP antibody. These constructs included wild-type, three missense variants and three stop-gain variants. Lane 1: untransfected cells; Lane 2: wild-type; lane 3: pLys649Arg; lane 4: pTyr763His; lane 5: pAsp997del; lane 6: pGly257*; lane 7: pGln398*; lane 8: pArg540*. This blot demonstrates that all ZMYM2-YFP-fusion proteins used for the BRET assays (wild-type, pGly257*, pGln398*, pArg540*) are expressed at the expected molecular weights.

Figure S10. Proximity-dependent biotin identification demonstrating the ZMYM2 protein interaction landscape or ZMYM2 interactome

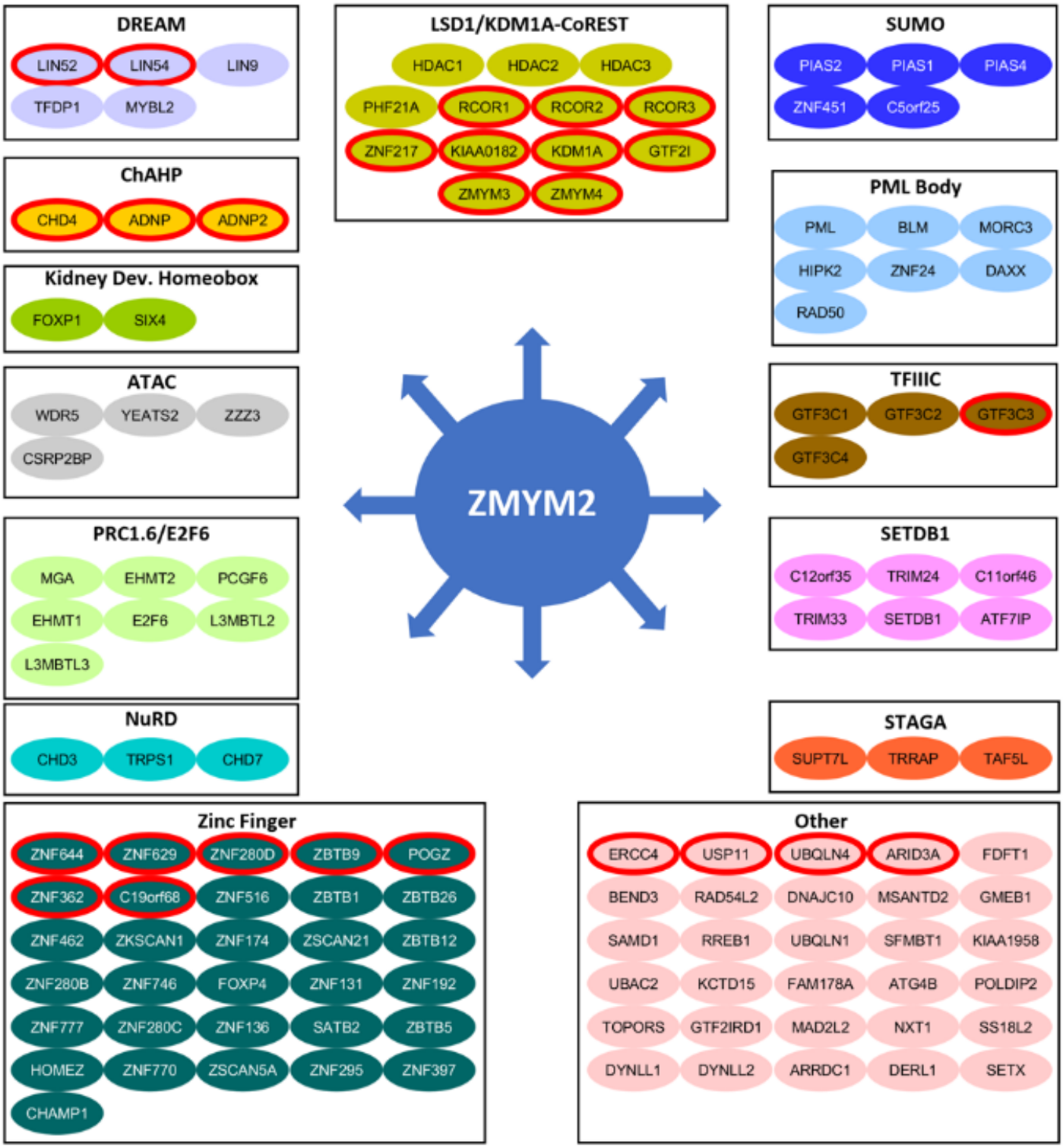

The interactome shows that ZMYM2 is significantly enriched in DNA binding transcription factors, transcriptional co-repressors, and proteins linked to chromatin regulation, chromatin organization and SUMO ligase activity (p=6.7x10-05). The majority of the components involved multiple previously reported ZMYM2 interactors26: LSD1(KDM1A)-CoREST (Corum complexes 633 and 1492)27, HDAC128 and HDAC2 (Corum 632). IP-MS (immunoprecipitation coupled with mass spectrometry) analyses were identified in our ZMYM2 BioID analysis (HDAC1, HDAC2, KDM1A/LSD1, GTF2I, GSE1/KIAA0182, PHF21A/BHC80, RCOR1, RCOR2, RCOR3, ZNF217, ZMYM3 and ZMYM4)

Figure S11 *ZMYM2* truncation mutant BioID Heat Map

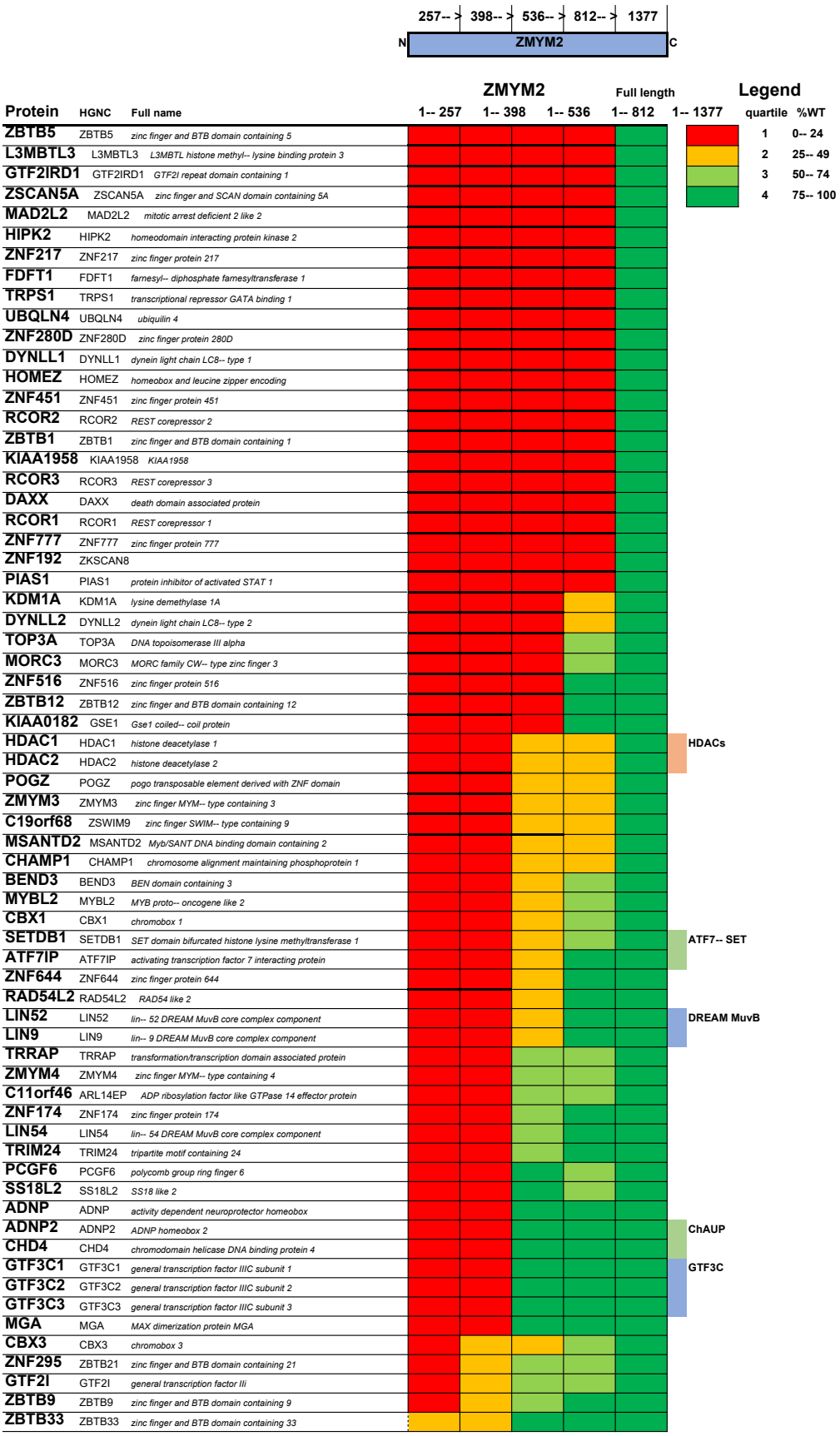

Table S1. List of mutagenesis primers used to generate clones representing the variants identified in each family

Family	Nucleotide change	Amino acid change	F: Forward primer R: Reverse primer
SSC1	c.181_183del	p.Val61del	F: aggttgtacaggttcgataaaaacatcatcatcatcttccac R: gtggaagatgatgatgatgtttttatcgaacctgtacaacct
A781	c.377A>C	p.Glu126Ala	F: ctcttgcccttgatttgttgccatgtcctcttcatcatc R: gatgatgaagaggacatggcaacaaatcaagggcaagag
GM10	c.622C>T	p. Arg208*	Not tested
GM1	c.766_767dupGT	p. Gly257*	F: gattaaaaggtcctacactccagtcttggtctgtgaagttaa R: ttaacttcacagaccaagactggagtgtaggacctttaatc
SSC2	c.1159A>G	p.Ile387Val	F: cttgaatccacttgagcaacaacggttcctttcattgtagttata R: tataactacaatgaaaggaaccgttgttgctcaagtggattcaag
GM3	c.1192C>T	p. Gln398*	F: gatgtactacagaattcctagaaggactcacttgaatcc R: ggattcaagtgagtccttctaggaattctgtagtacatc
GM16	c.1351C>T	p.His451Tyr	Not tested
GM15	c.1654A>G	p.I552V	Not tested
GM9	c.1367dup	p.Tyr456*	Not tested
SSC3	c.1607del	p.Cys536Leufs*13	F: tgttcggcaaccagtaaagttgtcagttttccatatttctc R: gagaaatatggaaaactgacaactttactggttgccgaaca
A4730 **A1204**	c.1618C>T	p. Arg540*	F: aaacctgcactgtgttcagcaaccagtacaagttg R: caacttgtactggttgctgaacacagtgcaggttt
GM11	c.1623_1627del	p.Cys543Valfs*3	Not tested
A3928	c.1946A>G	p.Lys649Arg	F: tccaggatttctggtcttgaacaaaaggaatttttgcagtagttg R: caactactgcaaaaattccttttgttcaagaccagaaatcctgga
GM17	c.2165T>A	p. Leu722*	Not tested
B1410	c.2287T>C	p.Tyr763His	F: cacaccttgcagccttgtggtaccaatcctgaaattt R: aaatttcaggattggtaccacaaggctgcaaggtgtg
A663/ A3135	c.2287_2288 delinsTA>CT	p.Tyr763Leu	F: cagtcacaccttgcagccttgaggtaccaatcctgaaatttttt R: aaaaaatttcaggattggtacctcaaggctgcaaggtgtgactg

B960	c.2324G>A	p.Gly775Glu	F: tgaactcgctctttaagagtttcttgagatttacaacagtcac R: gtgactgttgtaaatctcaagaaactcttaaagagcgagttca
GM19	c.2338C>T	p.Arg780*	Not tested
GM6	c.2434_2437del	p.Lys812Aspfs*18	F: gcccaacatgacaactcaggacctgaaaacttacatta R: taatgtaagttttcaggtcctgagttgtcatgttgggc
GM18	c.2494-1 G>A	IVS15-1 G>A	Not tested
SSC4	c.2990_2992 del	p.Asp997del	F: atctggttcatatggtacaggcatgctggactgt R: acagtccagcatgcctgtaccatatgaaccagat
SSC5	c.3091G>A	p.Glu1031Lys	F: ggctgttcctcatattctttgccaaaaacaggtggtaat R: attaccacctgtttttggcaaagaatatgaggaacagcc
GM7	c.3130_3131dup AA	p.Gly1045 Argfs*33	F: cccagacctcgatctaaaaaaaaaagggagccaagag R: ctcttggctccctttttttttagatcgaggtctggg
GM13	c.3176dup	p.Asp1059 Glufs*2	Not tested
GM12	c.3246G>A	p. Trp1082*	Not tested

Table S2. Twelve non-pathogenic missense heterozygous mutations in *ZMYM2* in 13 individuals from 12 families with congenital anomalies of the kidney and urinary tract

Family -Individual	Nucleotide change	Amino acid change[a, b]	Exon (Segre-gation)	Poly 2 SIFT MT	Amino acid conservation to species	gnomAD allele frequency[a]	Ethnicity Gender	CAKUT (sidedness[a])	Extra-renal manifestation	Neurologic involvement
SSC1 -21	c.181_183del	p.Val61del	3 *de novo*	/ / /	/	/	Poland M	UUT: Renal Agenesis (L)	Heart: ASD	-
A781 -21	c.377A>C	p.Glu126Ala	3 (ND)	0.16 Tol. /	*A.platyrhynchos*	/	Macedonia F	UUT: Duplex kidney (BL) LUT: Ureterocele (L)	Skeleton: Facial dysmorphism[1] Congenital hip dysplasia	-
SSC2 -21	c.1159A>G	p.Ile387Val	5 *de novo*	0.48 Tol. /	*D. rerio*	/	Italy M	UUT: UPJO (L)	Heart: WPW syndrome	-
GM16 -21	c.1351C>T	p.His451Tyr	8 p het m WT (imprinting)	0.81 Tol /	*D. rerio*	0/1/238682	?	-	Skeletal: Excessive femoral anteversion, gait disturbance Skin: Alopecia, Ectodermal dysplasia, , Other: Hyponatremia, Hypothyroidism, Ichthyosis, Neutropenia, Photophobia, Recurrent infections, Abnormal thrombosis, Thrombocytopenia	Global DD, Mild ID, Rotary nystagmus, Seizures
GM15 -21	c.1654A>G	p.I552V	10 *de novo*	0.103 Tol /	*D. rerio*	/	?	NA	Skeletal: Scoliosis	Macrocephaly, hypotonia, DD
A3928 -21	c.1946A>G	p.Lys649Arg	10 (ND)	0.98 Tol. /	*D. rerio*	/	Indian M	UUT: Renomegaly (BL)	-	-
B1410 -21	c.2287T>C	p.Tyr763His	12 p het m WT	0.90 Tol. /	*D. rerio*	0/**10**/240,574	Macedonia M	UUT: Hypoplastic pelvic kidney (L) LUT: Cryptorchidism (BL)	-	-
-11	c.2287T>C	p.Tyr763His	12 p het m WT	0.90 Tol. /	*D. rerio*	0/**10**/240,574	Macedonia M	**RUS-N** LUT: Cryptorchidism (BL)	-	-
A663 -21	c.2287_2288 delinsTA>CT	p.Tyr763Leu[b]	12 (ND)	0.21 Tol /	*D. rerio*	0/**10**/237,916	Kuwait F	UUT: Horseshoe kidney, UPJO (L)	-	-
A3135 -21	c.2287_2288 delinsTA>CT	p.Tyr763Leu[b]	12 (ND)	0.21 Tol /	*D. rerio*	0/**10**/237,916	Kuwait M	UUT: Horseshoe kidney, renal calculi	-	-
B960 -21	c.2324G>A	p.Gly775Glu	13 (p NA m WT)	1.00 Del /	*D. rerio*	0/1/245,306	Caucasian F	UUT: UPJO (BL), renal calculi	-	-
SSC4 -21	c.2990_2992 del	p.Asp997del	18 *de novo*	/ / /	/	/	Netherland M	UUT: Renal agenesis (L) LUT: Duplex urethra	Skeleton: Club hand, hemi-vertebrae (VACTERL)	-

SSC5-21	c.3091G>A	p.Glu1031Lys	19 *de novo*	0.07 Tol. /	*D. rerio*	0/0/225,618	Macedonia F	UUT: UVJO (R)	-	-

Transcript accession number for *ZMYM2* **NM_001190965.2 a** sidedness of CAKUT phenotype given in parentheses; ND denotes not done. ? denotes unknown.

ASD, atrial septal defect; **BL**, bilateral; **DD**; developmental delay; **Del**, deleterious; **F**, female; **het**, heterozygous; **ID**, intellectual disability; **L**, left; **LUT**, lower urinary tract; **m**, maternal; **M**, male; **N**, normal; **NA**, not available; **p**, paternal; **PPH2 score**, HumVar PolyPhen-2 prediction score; **R**, right; **RUS-N**, renal ultrasound normal; **SIFT**, sorting tolerant from intolerant; **Tol.**, tolerated; **UUT**, upper urinary tract; **UPJO**; ureteropelvic junction obstruction; **RUS**, renal ultrasound; **VACTERL**, vertebral defects, anal atresia, cardiac defects, tracheo-esophageal fistula, renal anomalies, and limb abnormalities.

Table S3. List of truncating heterozygous variants of *ZMYM2* that exist in gnomAD.

Note: In 31 truncating variants present in gnomAD 27 are only reported once heterozygously and never homozygously (see last column). This is consistent with the hypothesis that the CAKUT causing mutations outlined in Table 1 occurred *de novo* and with reduced transmission of truncating alleles due to a sub-fertility phenotype.

Gene	hg19 position	Type of mutation	Exon	Zygosity	c.change	p.change	SNP ID	Present in 1000-genomes	EVS	gnomAD (hom/het/allele count)
ZMYM2	chr13:20567212CA>C	5' UTR deletion (1 bp)	3 of 25	het	c.-1del	p.Met1?	rs769561518	/	/	0/4/230248
ZMYM2	chr13:20567337T>A	stop gained	3 of 25	het	c.125T>A	p.Leu42Ter		/	/	0/1/249444
ZMYM2	chr13:20567613AT>A	frameshift	3 of 25	het	c.403del	p.Ser135 ProfsTer31	rs767307088	/	/	0/1/249650
ZMYM2	chr13:20567936C>T	stop gained	3 of 25	het	c.724C>T	p.Gln242Ter				0/1/251188
ZMYM2	chr13:20580624T>A	stop gained	6 of 25	het	c.1410T>A	p.Cys470Ter	rs754728724	/	/	0/1/248728
ZMYM2	chr13:20580727G>A	splice donor	Intron 6	het	c.1512+1G>A	100% ESS				0/1/ 247968
ZMYM2	chr13:20580727G>T	splice donor	Intron 6	het	c.1512+1G>T	100% ESS				0/1/247968
ZMYM2	chr13:20593759G>A	splice donor	Intron 7	het	c.1584+1G>A	100% ESS		/	/	0/1/31384
ZMYM2	chr13:20608479_20608480del	frameshift	11 of 25	het	c.2054_2055del	p.Gln685 ArgfsTer7	rs1241090598			0/1/31396
ZMYM2	chr13:20608493_20608494del	frameshift	11 of 25	het	c.2068_2069del	p.Leu690 SerfsTer2	rs1474114489			0/1/245312
ZMYM2	chr13:20632845G>A	splice donor	Intron 15	het	c.2623+1G>A	100% ESS	rs766769611	/	/	0/1/248444
ZMYM2	chr13:20632988G>T	splice acceptor	Intron 15	het	c.1070-1G>T					0/1/226006
ZMYM2	chr13:20632998G>A	stop gained	Intron 15	het	intronic	p.Trp360Ter		/	/	0/2/220922
ZMYM2	chr13:20633039CTG>C	frameshift	Intron 15	het	intronic	p.Leu374HisfsTer12		/	/	0/1/176838
ZMYM2	chr13:20635344C>CA	frameshift	17 of 25	het	c.2892dup	p.Glu965 ArgfsTer11		/	/	0/1/248630
ZMYM2	chr13:20641009G>GT	frameshift	20 of 25	het	c.3152dup	p.Ser1052 IlefsTer7	rs778985497	/	/	0/1/236934
ZMYM2	chr13:20641049C>A	stop gained	20 of 25	het	c.3191C>A	p.Ser1064 Ter	rs769681794	/	/	0/1/248184
ZMYM2	chr13:20641051GA>G	frameshift	20 of 25	het	c.3195del	p.Glu1065 AspfsTer12		/	/	0/1/248352
ZMYM2	chr13:20641151T>G	stop gained	20 of 25	het	c.3293T>G	p.Leu1098 Ter	rs756477730	/	/	0/1/237798
ZMYM2	chr13:20641159TGTAA>T	splice donor	Intron 20	het	c.3301+3_3301+6delAA...	-79.4% SS	rs745854601	/	/	0/1/230760
ZMYM2	chr13:20641160G>C	splice donor	Intron 20	het	c.3301+1G>C	100% ESS		/	/	0/1/230574

Gene	hg19	Type	Exon	Zygos-ity	c.change	p.change	SNP ID	In '1000-genomes'?	EVS	gnomAD (hom/het/allele count)
ZMYM2	chr13:20641465C>T	stop gained	21 of 25	het	c.3388C>T	p.Arg1130 Ter	rs1299725201			0/1/242044
ZMYM2	chr13:20656154_20656155del	splice acceptor	21 of 25	het	c.34542_3454-1delAG	100% ESS	rs1176659089	/	/	0/4/191222
ZMYM2	chr13:20656154A>T	splice acceptor	21 of 25	het	c.3454-2A>T	100% ESS	rs1408869997			0/18/198980
ZMYM2	chr13: 20656155G>T	splice acceptor	21 of 25	het	c.3454-1G>T	100% ESS	rs1421349760			0/21/213812
ZMYM2	chr13:20657015C>CT	frameshift	23 of 25	het	c.3666dup	p.Asn1223 Ter		/	/	0/1/249220
ZMYM2	chr13:20657101AT>A	frameshift	23 of 25	het	c.3750del	p.Pro1251 LeufsTer2		/	/	0/1/31406
ZMYM2	chr13:20657133C>T	stop gained	23 of 25	het	c.3781C>T	p.Arg1261 Ter	rs773436243	/	/	0/1/248642
ZMYM2	chr13:20657897G>T	stop gained	24 of 24	het	c.3922G>T	p.Glu1308 Ter	rs1241191383	/	/	0/1/233828
ZMYM2	chr13:20660054C>G	stop gained	25 of 25	het	c.4034C>G	p.Ser1345 Ter	rs1429293566			0/1/249166
ZMYM2	chr13:20660104_20660105insG	frameshift	25 of 25	het	c.4084_4085 insG	p.Lys1362 ArgfsTer5	rs774438077			0/1/249016

bp, base pair; Del, deletion; ESS, essential splice site; EVS, exome variant server; het, heterozygous; hom, homozygous; ins, insertion; SNP, single nucleotide polymorphism; UTR, untranslated region.

Table S4A. Overview of *ZMYM2* variants identified in two control cohorts of 100 families with steroid resistant nephrotic syndrome and 238 families with nephronophthisis.

COHORT	TRUNCATING VARIANTS	MISSENSE VARIANTS	INFRAME VARIANTS
SRNS solved (n=100)	0	2	0
NPHP unsolved (n=238)	0	2	0

SRNS, steroid resistant nephrotic syndrome; NPHP, nephronophthisis.

Table S4B. Overview of monogenic causes identified in a cohort of 100 patients with steroid resistant nephrotic syndrome.

Gene	OMIM ID	Mode of inheritance	Percentage of patients (%)
ADCK4	#615567	AR	3
AGXT	#604285	AR	2
CLCN5	#300008	XL	1
COL4A3	#120070	AR, AD	7
COL4A4	#120131	AR, AD	2
COL4A5	#303630	XL	3
COQ2	#609825	AR	1
CTNS	#219800	AR	1
DGKE	#601440	AR	1
GLA	#300644	XL	1
INF2	#610982	AD	2
ITGA3	#605025	AR	1
KANK4	#614612	?AR	1
LAMB2	#150325	AR	6
LMX1B	#602575	AD	2
MYO1E	#601479	AR	3
NPHS1	#256300	AR	12
NPHS2	#600995	AR	12
NUP107	#607617	AR	1
NUP205	#614352	AR	2
NUP93	#614351	AR	3
OSGEP	#610107	AR	3
PDSS2	#610564	AR	1
PLCE1	#608414	AR	10
RPL15	#604174	AD	1
SGPL1	#603729	AR	3
SMARCAL1	#606622	AR	7
TRPC6	#603652	AD	1
TTC21B	#612014	AR, AD	2
WDR73	#616144	AR	3
WT1	#607102	AD	2

AR, autosomal recessive; AD, autosomal dominant; XL; X-linked